The Astrophysical Journal Letters, 725:L172–L175, 2010 December 20 doi:10.1088/2041-8205/725/2/L172

THE HDO/H_2O RATIO IN GAS IN THE INNER REGIONS OF A LOW-MASS PROTOSTAR

Jes K. Jørgensen[1] and Ewine F. van Dishoeck[2,3]
[1] Centre for Star and Planet Formation, Natural History Museum of Denmark, University of Copenhagen, Øster Voldgade 5-7, DK-1350 Copenhagen K., Denmark; jes@snm.ku.dk
[2] Leiden Observatory, Leiden University, P.O. Box 9513, NL-2300 RA Leiden, The Netherlands
[3] Max-Planck Institut für extraterrestrische Physik, Giessenbachstrasse, D-85748 Garching, Germany; ewine@strw.leidenuniv.nl
Received 2010 October 13; accepted 2010 November 8; published 2010 December 1

ABSTRACT

The HDO/H_2O abundance ratio is thought to be a key diagnostic for the evolution of water during the star and planet formation process and thus for its origin on Earth. We here present millimeter-wavelength high angular resolution observations of the deeply embedded protostar NGC 1333-IRAS4B from the Submillimeter Array targeting the 3_{12}–2_{21} transition of HDO at 225.6 GHz ($E_u = 170$ K). We do not (or only very tentatively) detect the HDO line toward the central protostar, contrasting the previous prominent detection of a line from another water isotopologue, $H_2^{18}O$, with similar excitation properties using the IRAM Plateau de Bure Interferometer. The non-detection of the HDO line provides a direct, model-independent, upper limit to the HDO/H_2O abundance ratio of 6×10^{-4} (3σ) in the warm gas associated with the central protostar. This upper limit suggests that the HDO/H_2O abundance ratio is not significantly enhanced in the inner ≈50 AU around the protostar relative to what is seen in comets and Earth's oceans and does not support previous suggestions of a generally enhanced HDO/H_2O ratio in these systems.

Key words: astrochemistry – ISM: abundances – ISM: individual objects (NGC 1333-IRAS4B) – protoplanetary disks – stars: formation

Online-only material: color figure

1. INTRODUCTION

One of the key questions concerning the formation of planets, and Earth in particular, is how water has evolved on its way from collapsing molecular cloud cores to protoplanetary disks and *eventually* Earth's oceans. In cold and quiescent regions, the gas-phase water abundance is low, only 10^{-9} to 10^{-8} or less (e.g., Bergin & Snell 2002; Caselli et al. 2010), but in regions forming low-mass protostars with intense heating or active shocks, its abundance can reach 10^{-4} with respect to H_2—comparable to or higher than that of CO (e.g., Kristensen et al. 2010). Thus, in the earliest prestellar stages and in large parts of the dense envelopes around low-mass protostars, H_2O is largely frozen out and is the dominant constituent of the icy mantles of dust grains. It is thought that the amount of deuterated relative to non-deuterated water is established in these grain mantles. Observations show that this abundance ratio is enhanced in comets (∼(3–4) × 10^{-4}; e.g., Bockelée-Morvan et al. 1998; Villanueva et al. 2009) and Earth's oceans (∼1.5 × 10^{-4}; e.g., Robert et al. 2000, and references therein) relative to primordial D/H ratio in the protosolar nebula (∼1.5 × 10^{-5}; Geiss & Gloeckler 1998; Linsky 2003). Determining when and where this ratio is established is thus a potentially important way to trace the evolution of water in the different stages of star formation. In particular, it might help determine what fraction of water was brought to Earth at later times through cometary impacts compared to being accreted during the formation of the planet itself (e.g., Morbidelli et al. 2000; Raymond et al. 2004) and whether water undergoes significant processing in warm regions of protostellar envelopes or disks before reaching newly formed planets.

Previous attempts at measuring the ratio of HDO and H_2O in low-mass protostars have had mixed success. Direct attempts to detect HDO in the solid phase at infrared wavelengths have provided upper limits of [HDO]/[H_2O] varying from 0.005 to 0.02 in a sample of protostars (Parise et al. 2003), which are not strong constraints compared to the two orders of magnitude lower abundance ratios observed in, e.g., the cometary systems. Measurements at (sub)millimeter wavelengths could potentially be sensitive to lower abundances of HDO in the gas phase in regions where the ices have evaporated off the dust grains and thus trace their compositions indirectly, but such measurements are complicated due to the achievable angular resolution using single-dish radio telescopes and have led to discrepant results. As an example, Stark et al. (2004) and Parise et al. (2005) analyzed the HDO emission toward the deeply embedded protostar, IRAS 16293-2422, compared to previous *Infrared Space Observatory* (*ISO*) and *Submillimeter Wave Astronomy Satellite* (*SWAS*) observations of non-deuterated H_2O. Both presented detailed models for the HDO abundance structure with significantly different results: Parise et al. found evidence for a drop in the [HDO]/[H_2O] ratio from 0.03 in the hot gas in the inner envelope (i.e., significantly enhanced above the cometary values) to <0.002 in the cold gas on larger scales, whereas Stark et al. in contrast found that the abundance of HDO was best described as being constant throughout the envelope and with an [HDO]/[H_2O] ratio of 2×10^{-4}, comparable to the cometary value, in the part of the envelope with $T > 14$ K. Part of this discrepancy may arise due to the complexities in comparisons between ground-based single-dish observations of HDO and space-based observations of H_2O probing significantly different spatial scales, and lines excited in different regions of the protostellar environment.

Our detection of thermal $H_2^{18}O$ emission toward the deeply embedded Class 0 low-mass protostar, NGC 1333-IRAS4B ($d = 250$ pc), with the IRAM Plateau de Bure Interferometer (Jørgensen & van Dishoeck 2010) makes it possible to revisit the discussion of the origin of water on Earth, namely, where the relative abundances of deuterated and non-deuterated are established. In this Letter, we present a search for the 225.9 GHz 3_{12}–2_{21} transition of the HDO isotopologue at high angular resolution (2.5″–3″; corresponding to 625–700 AU) using the

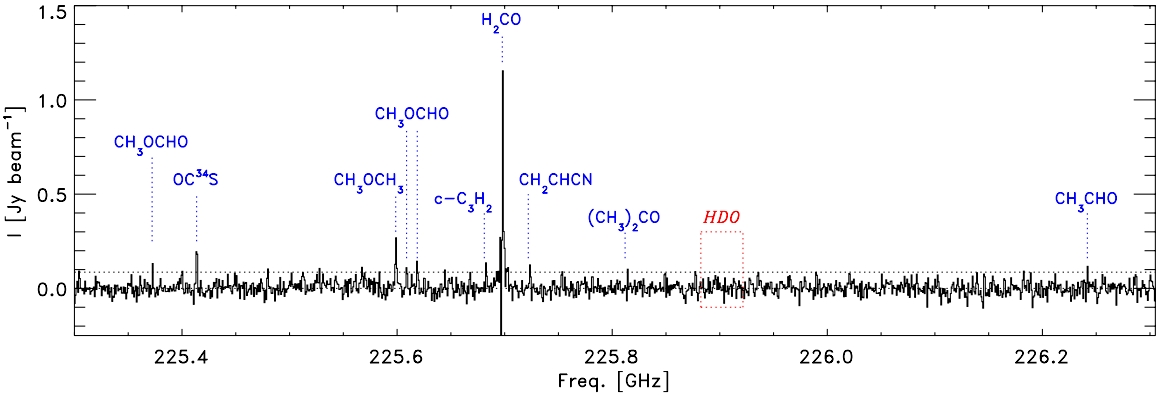

Figure 1. Spectrum extracted in the central 3.″0 × 2.″5 beam toward the continuum position for IRAS4B. The detected lines are indicated at the position of their catalog rest frequency corrected for the 7.0 km s^{-1} systemic velocity of IRAS4B. The box shows the zoom-in around the HDO $3_{1,2}$–$2_{2,1}$ transition displayed in Figure 2; the high spectral resolution chunk including this line has been rebinned to the same 1.1 km s^{-1} spectral resolution as for the other chunks in the wider bands. The horizontal dotted lines indicate the zero and 3σ levels.

(A color version of this figure is available in the online journal.)

Table 1
Parameters for IRAS4B and IRAS4B′ from Elliptical Gaussian Fits to Their Continuum Emission

Parameter	IRAS4B	IRAS4B′
Flux	1.021 Jy	0.364 Jy
R.A. (J2000)	03:29:12.0	03:29:12.8
Decl. (J2000)	31:13:08.1	31:13:06.9
Extent[a]	1.″7 × 0.″96 (−68°)	1.″6 × 0.″91 (+55°)

Note. [a] Size of Gaussian from fit in (u, v)-plane (i.e., deconvolved FWHM size) and position angle of major axis (in parentheses).

Submillimeter Array (SMA). This transition is close in energy to the $H_2^{18}O$ 3_{13}–2_{20} transition from Jørgensen & van Dishoeck (2010) (E_{up} = 170 K versus 204 K) and a straightforward comparison can thus be made between these species with minimal uncertainties due to their excitation properties.

2. OBSERVATIONS

We observed NGC 1333-IRAS4B (IRAS4B in the following; α = 03^{h}29^{m}12.00^s., δ = +31^{d}13′08.″1 [J2000] Jørgensen et al. 2007) using the SMA (Ho et al. 2004) on 2008 October 31. The receivers were tuned to the HDO $3_{1,2}$–$2_{2,1}$ transition at 225.89672 GHz and the SMA correlator assigned a chunk with 512 channels centered on this line corresponding to a 0.27 km s^{-1} spectral resolution over about 100 MHz of the chunk. The chunk was placed so that the upper sideband covered the D_2CO transition at 236.102128 GHz with similar spectral resolution. For the remaining SMA passband 128 channels were allocated in each chunk giving a uniform spectral coverage of 1.1 km s^{-1} from 225.0 to 227.0 GHz (lower sideband, LSB) and 235.0 to 237.0 GHz (upper sideband, USB). The source was observed in the compact configuration of the SMA, which at the time of observations had seven antennae operational providing baselines ranging from 7 to 60 kλ.

The data were calibrated using the SMA version of the MIR package and imaged using Miriad. The calibration followed the standard approach: the absolute flux calibration was established through observations of Uranus, the bandpass by observations of the strong quasar 3c454.3, and the complex gains by regular observations of the nearby strong quasars 3c84 and 3c111 (approximately 5.2 and 4.7 Jy at 1.33 mm, respectively). Integrations with clearly deviating amplitudes and/or phases were flagged and the continuum was subtracted prior to Fourier transformation of the line data. With natural weighting the resulting beam size is 3.″1 × 2.″5 at a position angle of −66°; the field of view is 52″ (HPBW) at 1.33 mm. The resulting rms noise level is 58 mJy beam^{-1} channel^{-1} for the line data with the 0.27 km s^{-1} spectral resolution using natural weighting.

3. RESULTS

Both IRAS4B and its nearby companion IRAS4B′ are clearly detected in the continuum data. Table 1 lists the results of elliptical Gaussian fits to the two sources: both are resolved with fluxes in agreement with the results from Jørgensen et al. (2007) within the absolute flux calibration uncertainty of 20%.

Figure 1 shows the spectrum from 1 GHz of the LSB of IRAS4B labeling a number of lines with peaks at the 3σ level or above. The H_2CO $3_{1,2}$–$2_{1,1}$ transition at 225.698 GHz is clearly dominant as expected, with lines of complex organic molecules as well as $OC^{34}S$ and c-C_3H_2 also detected. Most importantly the identification of the multiple lines centered at the continuum position confirms both the pointing of the observations as well as the calibration of the frequency axes of the spectra.

Figure 2 shows a zoom-in on the spectrum in the high resolution chunk around the HDO $3_{1,2}$–$2_{2,1}$ transition. No clear line is seen at the systemic velocity of 7.0 km s^{-1} of the $H_2^{18}O$ $3_{1,3}$–$2_{2,0}$ transition (Jørgensen & van Dishoeck 2010) and other species surveyed at high angular resolution with the SMA (Jørgensen et al. 2007)—although a tentative detection may be present at the ≈3σ level (integrated intensity). This is confirmed by the integrated intensity map (Figure 2, right), which shows a 3σ contour close to the location of the continuum peak. Statistically speaking it cannot be counted a firm detection, however, and we therefore treat it as an upper limit in the following.

4. DISCUSSION: AN UPPER LIMIT ON THE RATIO OF THE HDO/H_2O ABUNDANCES IN THE INNER 50 AU REGIONS OF A LOW-MASS PROTOSTAR

The 3σ upper limit on the integrated line intensity (or approximate strength of the tentative detection) of the HDO transition can be estimated as $3\sigma_{int} = 3\sqrt{\Delta v\, \delta v}\, \sigma_{rms} \approx 0.13$ Jy km s^{-1}, assuming a line width to zero intensity of 2 km s^{-1} as found for the $H_2^{18}O$ transition. The column density of HDO corresponding

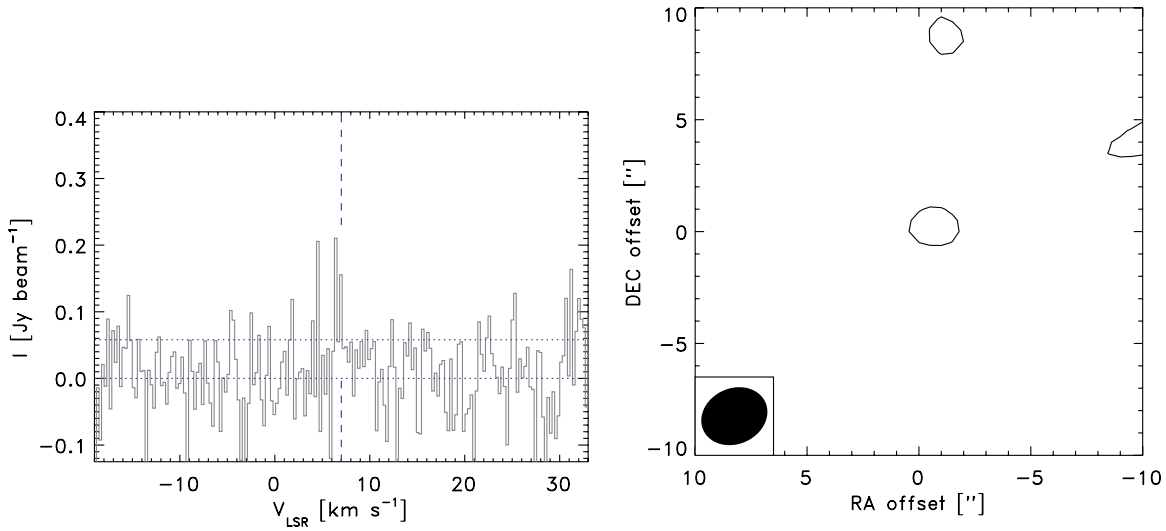

Figure 2. Left: spectrum centered on the expected location of the HDO $3_{1,2}$–$2_{2,1}$ transition. The dotted lines indicate the zero and 1σ levels. The dashed line, the expected location of the HDO line at the systemic velocity of the $H_2^{18}O$ $3_{1,3}$–$2_{2,0}$ transition, and other species at 7.0 km s^{-1}. Right: integrated intensity of the data cube over ±1 km s^{-1} around the expected location of the HDO transition. The contour corresponds to the 3σ level (no emission is seen at 4σ levels or higher).

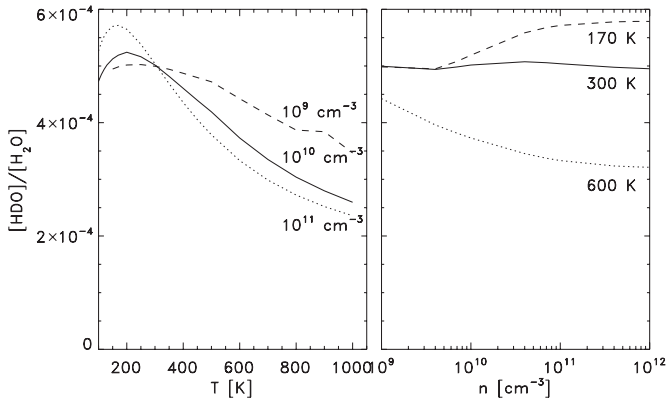

Figure 3. Estimates of the HDO/H_2O abundance ratio as function of temperature (left) and density (right) from non-LTE Radex calculations. Each panel shows three curves: in the left panel for constant densities of 10^9 cm^{-3}, 10^{10} cm^{-3}, and 10^{11} cm^{-3} and in the right panel for constant temperatures of 170 K, 300 K, and 600 K.

to this intensity can be estimated under the same assumptions as for the $H_2^{18}O$ transition and can thus be compared directly, assuming that the emission is optically thin and uniform over the extent of the $H_2^{18}O$ emission (thus diluted in our SMA beam).

Using the non-LTE escape probability code Radex (van der Tak et al. 2007), we calculated column densities corresponding to the observed line intensities for different values of the kinetic temperature and H_2 density. Figure 3 shows the derived HDO/H_2O abundance ratio as function of kinetic temperature and density, respectively. In the range from about 100 to 1000 K and for densities larger than about 10^9 cm^{-3} (the density expected in the inner envelope or disk) the derived [HDO]/[H_2O] 3σ upper limit on the abundance ratio varies from about 2×10^{-4} to 6×10^{-4} assuming an ortho–para ratio for $H_2^{18}O$ of 3:1 and a $^{16}O/^{18}O$ ratio of 560. If the tentative detection would be confirmed by more sensitive observations, the implied HDO/H_2 abundance ratio would suggest a level of deuteration comparable to what is observed in cometary ices. The Radex calculations show that the inferred abundance ratio can vary from about 1×10^{-4} to 1×10^{-3} if the excitation temperatures are allowed to differ for the two species and vary between 100 and 1000 K, covering a wider range of physical parameters. The beauty of the above result is that it does not depend on the assumed physical structure of the source, and in particular, whether the origin of the observed water is due to shocks or ice desorption in either envelope or disk material.

One caveat is that the $H_2^{18}O$ transition could be masing as is the case for the same transition of main $H_2^{16}O$ isotopologue at 183 GHz (e.g., Cernicharo et al. 1994). In that scenario the $H_2^{18}O$ column density would be overestimated and thus the [HDO]/[H_2O] ratio underestimated. A few observational facts argue against this being a major issue for the $H_2^{18}O$ transition toward IRAS4B, though: the width of the $H_2^{18}O$ transition (2 km s^{-1} to zero-intensity) is very close to those of the other species (SO_2, C_2H_5CN, and CH_3OCH_3) observed in the central beam toward the continuum peak of IRAS4B. This trend is further strengthened with detections of the $H_2^{18}O$ transition toward two other embedded protostars (M. Persson et al. 2011, in preparation): the lines of $H_2^{18}O$, SO_2, and the organic species in these three sources show smaller species-to-species variations than source-to-source variations both in terms of their line widths and strengths. This suggests that the origin of the emission is the same in each of the individual sources and therefore that $H_2^{18}O$ emission is dominated by the thermal component and at most weakly masing. Finally, previously detected H_2O water masers at 22 GHz in IRAS4B are clearly offset from the systemic velocity (Marvel et al. 2008; Desmurs et al. 2009) and their motions in the outflow propagation direction are perpendicular to the tentative velocity gradient observed in the $H_2^{18}O$ transition. Thus, the $H_2^{18}O$ line is at least not masing in the gas where the 22 GHz H_2O maser has its origin.

The derived upper limit to the HDO/H_2O abundance ratio does not support the suggestion by Ceccarelli et al. (2005) and Parise et al. (2005) that the HDO/H_2O abundance ratio is abnormally high in low-mass protostars or their disks compared to the abundance ratios found in comets, Earth's oceans, or in high-mass hot core regions (e.g., Jacq et al. 1990; Gensheimer et al. 1996; van der Tak et al. 2006). In agreement with Stark et al. (2004), the results favor a scenario in which the HDO/H_2O ratio is conserved during the star formation process. There is thus also no need to invoke the formation of water in the gas phase

in a longer-lived early stage of low-mass protostars where the deuterium fractionation is too high to explain the constraints on the HDO/H_2O abundance ratio. The conclusion that the HDO/H_2O abundance ratio is determined in the cold core phase and is conserved throughout the formation of low-mass stars and icy solar-system bodies is consistent with the evolutionary models of Visser et al. (2009) that show that the bulk of the ice remains in solid form during infall and disk formation. It is possible that the physical mechanisms for the origin of the warm gas in NGC 1333–IRAS4B and IRAS 16293–2422 differ: the latter source shows a complex structure with multiple organic species peaking at different locations (e.g., Kuan et al. 2004; Bisschop et al. 2008) and likely interaction with the protostellar outflow on small scales (Chandler et al. 2005). SMA observations of that source (J. K. Jørgensen et al. 2011, in preparation) suggest that this complex interplay could also have an impact on the line emission for the HDO isotopologue underlining the need for high angular resolution observations.

In any case, these observations show the great potential offered by high angular resolution submillimeter (interferometric) observations, even from the ground, for tracing the origin and evolution of water vapor during the evolution of young stars. An important step forward would be to spatially resolve both the emission profiles of HDO and $H_2^{18}O$ in protostars in different evolutionary stages to reveal any temporal or spatial variations of their abundance ratios. More sensitive observations with the Plateau de Bure as well as future observations with the Atacama Large Millimeter Array in Band 5 will make this possible and thereby make an important contribution toward answering the questions about the origin of water in planetary systems.

We are grateful to Tim van Kempen for helpful comments about the manuscript. Research at Centre for Star and Planet Formation is funded by the Danish National Research Foundation and the University of Copenhagen's programme of excellence. Research in astrochemistry in Leiden is supported by a Spinoza Grant from the Netherlands Organization for Scientific Research (NWO) and a NOVA grant. This Letter is based on data from the Submillimeter Array: the Submillimeter Array is a joint project between the Smithsonian Astrophysical Observatory and the Academia Sinica Institute of Astronomy and Astrophysics and is funded by the Smithsonian Institution and the Academia Sinica.

REFERENCES

Bergin, E. A., & Snell, R. L. 2002, ApJ, 581, L105
Bisschop, S. E., Jørgensen, J. K., Bourke, T. L., Bottinelli, S., & van Dishoeck, E. F. 2008, A&A, 488, 959
Bockelée-Morvan, D., et al. 1998, Icarus, 133, 147
Caselli, P., et al. 2010, A&A, 521, L29
Ceccarelli, C., Dominik, C., Caux, E., Lefloch, B., & Caselli, P. 2005, ApJ, 631, L81
Cernicharo, J., Gonzalez-Alfonso, E., Alcolea, J., Bachiller, R., & John, D. 1994, ApJ, 432, L59
Chandler, C. J., Brogan, C. L., Shirley, Y. L., & Loinard, L. 2005, ApJ, 632, 371
Desmurs, J., Codella, C., Santiago-García, J., Tafalla, M., & Bachiller, R. 2009, A&A, 498, 753
Geiss, J., & Gloeckler, G. 1998, Space Sci. Rev., 84, 239
Gensheimer, P. D., Mauersberger, R., & Wilson, T. L. 1996, A&A, 314, 281
Ho, P. T. P., Moran, J. M., & Lo, K. Y. 2004, ApJ, 616, L1
Jacq, T., Walmsley, C. M., Henkel, C., Baudry, A., Mauersberger, R., & Jewell, P. R. 1990, A&A, 228, 447
Jørgensen, J. K., & van Dishoeck, E. F. 2010, ApJ, 710, L72
Jørgensen, J. K., et al. 2007, ApJ, 659, 479
Kristensen, L. E., et al. 2010, A&A, 521, L30
Kuan, Y., et al. 2004, ApJ, 616, L27
Linsky, J. L. 2003, Space Sci. Rev., 106, 49
Marvel, K. B., Wilking, B. A., Claussen, M. J., & Wootten, A. 2008, ApJ, 685, 285
Morbidelli, A., Chambers, J., Lunine, J. I., Petit, J. M., Robert, F., Valsecchi, G. B., & Cyr, K. E. 2000, Meteorit. Planet. Sci., 35, 1309
Parise, B., Simon, T., Caux, E., Dartois, E., Ceccarelli, C., Rayner, J., & Tielens, A. G. G. M. 2003, A&A, 410, 897
Parise, B., et al. 2005, A&A, 431, 547
Raymond, S. N., Quinn, T., & Lunine, J. I. 2004, Icarus, 168, 1
Robert, F., Gautier, D., & Dubrulle, B. 2000, Space Sci. Rev., 92, 201
Stark, R., et al. 2004, ApJ, 608, 341
van der Tak, F. F. S., Black, J. H., Schöier, F. L., Jansen, D. J., & van Dishoeck, E. F. 2007, A&A, 468, 627
van der Tak, F. F. S., Walmsley, C. M., Herpin, F., & Ceccarelli, C. 2006, A&A, 447, 1011
Villanueva, G. L., Mumma, M. J., Bonev, B. P., Di Santi, M. A., Gibb, E. L., Böhnhardt, H., & Lippi, M. 2009, ApJ, 690, L5
Visser, R., van Dishoeck, E. F., Doty, S. D., & Dullemond, C. P. 2009, A&A, 495, 881